PHILOSOPHICAL TRANSACTIONS OF THE ROYAL SOCIETY A MATHEMATICAL, PHYSICAL & ENGINEERING SCIENCES

Free Tidal Oscillations in Rotating Flat Basins of the Form of Rectangles and of Sectors of Circles

A. Pnueli and C. L. Pekeris

Phil. Trans. R. Soc. Lond. A 1968 **263**, 149-171
doi: 10.1098/rsta.1968.0009

FREE TIDAL OSCILLATIONS IN ROTATING FLAT BASINS OF THE FORM OF RECTANGLES AND OF SECTORS OF CIRCLES

By A. PNUELI and C. L. PEKERIS

Department of Applied Mathematics, The Weizmann Institute, Rehovot, Israel

(*Communicated by Sir Geoffrey Taylor, F.R.S.—Received* 31 *July* 1967)

A study is made of the periods of free tidal oscillations and of the corresponding wave patterns in rotating flat basins which have the form of rectangles or of sectors of circles. The analysis is based on a variational principle for tidal oscillations. It is shown that, if ζ denotes the tide height and ζ^* its complex conjugate, the sign of the integral $i\int\zeta^*(\mathrm{d}\zeta/\mathrm{d}s)\,\mathrm{d}s$, which is real, taken around the periphery of the basin, determines whether the tidal wave propagates around the basin in the direction of rotation (positive wave), or opposite to it (negative wave). The sense of propagation can also be told from the sign of $\mathrm{d}k^2(\tau)/\mathrm{d}\tau$, where $k^2 = (\sigma^2-4\omega^2)/gh$ and $\tau = 2\omega/\sigma$, ω denoting the speed of rotation, and σ the frequency. A discussion is given of the removal by rotation of the degeneracy that exists in some modes in the absence of rotation. The method (A) of expansion of ζ in terms of the eigenfunctions for no rotation ($\tau = 0$) was found to converge well only for $\tau \ll 1$. Our calculations were carried out by an adaptation of Trefftz's method, in which the variation of the surface integral is reduced to a variation of a line-integral taken along the boundary. This method (B) was found to be effective for all ranges of rotation. The solutions obtained illustrate that in some modes the tides are always positive, while in others they start out being negative at slow rotation and turn positive as the rotation is increased. A theory is developed, for basins of general shape, showing that as the speed of rotation is increased indefinitely a Kelvin regime sets in, in which the tide concentrates near the periphery, decreasing exponentially towards the interior. The Kelvin wave is positive and the characteristic frequencies σ_n are given by $\sigma_n = 2\pi n\sqrt{(gh)}/p$, p denoting the perimeter of the basin. It is shown that near a blunt corner of the coast the tide has a singularity like that in potential flow.

1. Introduction

In this investigation we present a general theory of the free tidal oscillations of rotating flat basins having the form of rectangles and of circular sectors. Our aim has been to gain insight into the dynamics of tides in these simple basins so as to serve as a guide in the interpretation of tidal studies in the more complicated real world oceans. In the latter, the approach is necessarily numerical, requiring the adoption of a rectangular grid for the finite difference method. The resulting jagged representation of the coastline was found to retard the convergence of the solution, and the question arises as to the theoretical distribution of the tide around a blunt corner such as is shown in figures 16 to 21. Our analysis shows that near a corner of angular opening π/μ ($\mu<1$), the tide height ζ is singular, as in potential flow, and is approximated by equation (95), where $\tau = 2\omega/\sigma$. Here ω denotes the angular rotation of the basin and σ the frequency of tidal oscillation. The degree of approximation attained by representation (95) is shown in table 1.

In the spectral analysis of the tidal oscillations, where the characteristic frequencies $\sigma_n(\omega)$ are determined as functions of the angular rotation ω, we found that a more meaningful

Vol. 263. A. 1138. (Price 12*s*. 6*d*.; U.S. $1.60) 19 [Published 13 June 1968

parameterization is the function $k_n^2(\tau)$, where $k_n^2 = (\sigma_n^2 - 4\omega^2)/gh$, and h denotes the depth of the liquid. These characteristic frequency functions $k_n^2(\tau)$ are shown in figures 2, 9, 15 and 22 for model basins of various shapes. From a variational formulation of the tidal problem given in equation (13) we deduce in § 4 that the slope of the $k^2(\tau)$ function determines the direction of propagation of the tidal wave. When $dk^2/d\tau > 0$, the wave is negative and advances in a direction opposite to that of the rotation of the basin, and vice versa when $dk^2/d\tau < 0$. As seen in figure 2 for a quadrant circular sector, the $k^2(\tau)$ curve for the first mode (I) has a negative slope everywhere, and the wave is therefore positive at all speeds of rotation. This is shown in the flow patterns in figures 3, 4 and 5, arranged in order of increasing speed of rotation. The $k^2(\tau)$ curve for mode II in figure 2 starts out with a positive slope, and the corresponding wave, shown in figure 6, is *negative*. As the maximum in curve II is passed, the originally negative wave is transformed into a positive one, as is illustrated in figures 7 and 8. This phenomenon of the transformation of an initially negative wave into a positive one was first demonstrated by Corkan & Doodson (1952), in connexion with Taylor's conjecture (Taylor 1922) that the tidal waves in a rectangular basin are always positive. For the case of a square basin, we seen from figure 22 that many of the waves are of the type that start out being negative at slow rotation, and become positive as the rotation is increased. Beyond the maximum in the $k^2(\tau)$ curve, the total change of phase as the wave makes a complete turn around the periphery of the basin is $2\pi n$, where n denotes the order of the mode.

As the speed of rotation is increased and k^2 becomes negatively large, the tidal wave tends to concentrate near the periphery of the basin, with very little motion remaining in the interior. The highest co-range lines tend then to assume a shape conforming to the coastline, as shown in figures 11, 13, 19, 21, and very prominently in 31. The tidal motion then consists of a Kelvin wave (Lamb 1932, § 208), progressing in the positive direction around the periphery of the basin. The theory of the establishment of a Kelvin regime in the free tidal oscillations of rotating basins of arbitrary shape is developed in § 6. It is shown there that the frequency σ_n in the Kelvin regime is given by $\sigma_n = 2\pi n\sqrt{(gh)}/p$, where p denotes the perimeter of the basin. The tidal amplitude decreases exponentially from the coast into the interior, as given by equation (44).

Our analysis is based on a variational formulation of the tidal problem, which is developed in § 2. Some results derivable from the variational formulation are summarized in § 3. In § 4 we prove that the sense of propagation of the tidal wave can be told from the sign of $dk^2(\tau)/d\tau$. The classification of the free tidal modes with respect to the direction of propagation of the wave and the degeneracy in the limit of no rotation is discussed in § 5. Our results, which are general, agree with the analysis made by Rao (1965, 1966) for the case of rectangular basins. Section 6 gives the theory of the Kelvin-type wave for flat basins.

In § 7 we discuss the efficacy of expanding the solution for the tide in the presence of rotation, in terms of the eigenfunctions for the case of no rotation (method A). It is found that the convergence becomes poor as the rotation parameter $\tau(= 2\omega/\sigma)$ becomes of the order of unity. Our calculations in this work were made by an adaptation of the method of Trefftz (Collatz 1965), whereby the tidal problem is reduced to a variational integral taken along the *boundary* of the basin. This method B is discussed in § 8. We found that where 50 terms were needed to assure convergence in method A, only 12 terms sufficed when method B

was used. The theory of free tidal oscillation in rectangular basins is developed in § 9 by method B. The case of basins of the shape of circular sectors is treated in § 10, also on the basis of method B.

2. Variational formulation of the tidal equations for flat basins

The tidal equations for flat basins, in the long wave approximation, are (Lamb 1932)

$$\frac{\partial u}{\partial t} - 2\omega v = -g\frac{\partial}{\partial x}(\zeta - \bar{\zeta}), \tag{1}$$

$$\frac{\partial v}{\partial t} + 2\omega u = -g\frac{\partial}{\partial y}(\zeta - \bar{\zeta}), \tag{2}$$

where u, v are the components of velocity in the directions x and y, ζ is the tidal elevation, and $\bar{\zeta}$ the equilibrium tide height given by

$$\bar{\zeta} = -\Omega/g, \tag{3}$$

with Ω denoting the tidal potential. The equation of continuity is

$$\frac{\partial \zeta}{\partial t} = -\frac{\partial}{\partial x}(hu) - \frac{\partial}{\partial y}(hv). \tag{4}$$

We shall be concerned here only with the *free* tidal oscillations, and shall also assume that the depth h is constant. With a time-factor $e^{i\sigma t}$, equations (1) and (2) can be solved for u and v in terms of ζ:

$$u = \frac{i\sigma g}{\sigma^2 - 4\omega^2}\left(\frac{\partial}{\partial x} - i\tau\frac{\partial}{\partial y}\right)\zeta, \tag{5}$$

$$v = \frac{i\sigma g}{\sigma^2 - 4\omega^2}\left(\frac{\partial}{\partial y} + i\tau\frac{\partial}{\partial x}\right)\zeta, \tag{6}$$

where

$$\tau = 2\omega/\sigma. \tag{7}$$

The equation of continuity (4) then yields the wave equation for ζ:

$$(\nabla^2 + k^2)\zeta = 0, \tag{8}$$

$$k^2 = \frac{\sigma^2 - 4\omega^2}{gh} = \frac{\sigma^2}{gh}(1 - \tau^2). \tag{9}$$

At a vertical boundary, the vanishing of the component of velocity normal to the boundary gives the boundary condition

$$\left(\frac{\partial}{\partial n} - i\tau\frac{\partial}{\partial s}\right)\zeta = 0, \tag{10}$$

where n denotes the outward normal to the boundary, and s the direction along the boundary.

The tidal wave equation (8) can be derived from the variational form

$$\delta\left\{\int\int [|\nabla\zeta|^2 - i\tau(\zeta_x^*\zeta_y - \zeta_x\zeta_y^*) - k^2|\zeta|^2]\,dA\right\} = 0, \tag{11}$$

whereupon equation (10) results as a *natural* variational boundary condition. Here the star denotes the complex conjugate. The variational formulation of the tidal equations for flat

basins was given by Lamb (1932, §205*b*, §212*a*), and for an ocean covering the rotating earth by Poincaré (1910). Using the relation

$$\iint (\zeta_x^* \zeta_y - \zeta_x \zeta_y^*)\, \mathrm{d}A = \int \zeta^* \frac{\partial \zeta}{\partial s}\, \mathrm{d}s, \tag{12}$$

we can transform (11) into

$$\delta\left\{\iint [|\nabla\zeta|^2 - k^2 |\zeta|^2]\, \mathrm{d}A - \mathrm{i}\tau \int \zeta^* \frac{\partial \zeta}{\partial s}\, \mathrm{d}s\right\} = 0. \tag{13}$$

The line-integral $\int \zeta^* (\partial\zeta/\partial s)\, \mathrm{d}s$ has an important physical interpretation. If we write for the tidal height $\zeta(s)$ on the boundary s

$$\zeta(s) = R(s) \exp\{\mathrm{i}[\sigma t + \theta(s)]\}, \tag{14}$$

then

$$-\mathrm{i} \int \zeta^* \frac{\partial \zeta}{\partial s}\, \mathrm{d}s = -\mathrm{i} \int R\dot{R}\, \mathrm{d}s + \int R^2 \frac{\mathrm{d}\theta}{\mathrm{d}s}\, \mathrm{d}s. \tag{15}$$

The first integral on the right vanishes, hence

$$-\mathrm{i} \int \zeta^* \frac{\partial \zeta}{\partial s}\, \mathrm{d}s = \int R^2 \dot{\theta}(s)\, \mathrm{d}s. \tag{16}$$

When $\dot{\theta}(s) < 0$ all along the boundary, the phase of the tide given in $\exp[\mathrm{i}(\sigma t + \dot{\theta}\Delta s)]$ represents a wave advancing along the boundary in the positive direction of increasing θ, whereas when $\dot{\theta}(s) > 0$, the wave advances in the negative direction. Hence, it follows that if the wave advances in the same direction all along the boundary, the direction of advance is positive or negative depending on whether the integral $\mathrm{i}\int \zeta^* (\mathrm{d}\zeta/\mathrm{d}s)\, \mathrm{d}s$ is positive or negative respectively.

3. Some consequences derivable from the variational formulation of the tidal equations

We shall state here some corollaries of the variational formulation of the tidal problem given in equation (13). The proofs, which will not be given here, can be made along the lines of the classical membrane theory, modified by the presence of the Coriolis τ-term in (13) and in the boundary condition (10).

1. The functional $D(\zeta)$ defined by

$$D(\zeta) = \iint |\nabla\zeta|^2\, \mathrm{d}A - \mathrm{i}\tau \int \zeta^* \frac{\partial \zeta}{\partial s}\, \mathrm{d}s, \tag{17}$$

is real.

2. A function ζ_1 which yields an extremum k_1^2 for $D(\zeta_1)$, subject to the normalization condition

$$H(\zeta_1) = \iint |\zeta_1|^2\, \mathrm{d}A = 1, \tag{18}$$

satisfies the wave equation

$$(\nabla^2 + k_1^2)\, \zeta_1 = 0, \tag{19}$$

and the *natural* boundary condition

$$\left(\frac{\partial}{\partial n} - \mathrm{i}\tau \frac{\partial}{\partial s}\right) \zeta_1 = 0. \tag{20}$$

In the case of the nth eigenvalue k_n, we have to impose on the eigenfunction ζ_n the additional condition of orthogonality to each of the eigenfunctions of lower order.

3. For all $\tau < 1$ $(\sigma > 2\omega)$, $D(\zeta)$ is positive. Hence for $\tau < 1$, the eigenvalues k_n^2 are discrete and positive.

4. The set of eigenfunctions ζ_n is complete and orthogonal

$$\int\int \zeta_i^* \zeta_j \, \mathrm{d}A = 0 \quad (i \neq j). \tag{21}$$

4. Determination of the direction of propagation of the tidal wave from the function $k^2(\tau)$

For a given value of τ, the system (8) and (10) has a set of eigenvalues $k_n^2(\tau)$. These eigenvalues will change continuously with the parameter τ, and will reduce to the eigenvalues for the case of no rotation as $\tau \to 0$. Let us examine the dependence of a given eigenvalue k^2 on τ. It can be shown that the associated eigenfunction ζ satisfies not only the variational equation (13), but also

$$\int\int |\nabla\zeta|^2 \, \mathrm{d}A - \mathrm{i}\tau \int \zeta^* \frac{\partial\zeta}{\partial s} \, \mathrm{d}s - k^2 \int\int |\zeta|^2 \, \mathrm{d}A = 0. \tag{22}$$

Differentiating (22) with respect to τ we get

$$-\mathrm{i}\int \zeta^* \frac{\partial\zeta}{\partial s} \, \mathrm{d}s - \frac{\mathrm{d}k^2}{\mathrm{d}\tau} \int\int |\zeta|^2 \, \mathrm{d}A + \left\{ \frac{\partial}{\partial\tau} \int\int |\nabla\zeta|^2 \, \mathrm{d}A - \mathrm{i}\tau \frac{\partial}{\partial\tau} \int \zeta^* \frac{\partial\zeta}{\partial s} \, \mathrm{d}s - k^2 \frac{\partial}{\partial\tau} \int\int |\zeta|^2 \, \mathrm{d}A \right\} = 0. \tag{23}$$

The term in brackets in (23) vanishes by (13), since it represents the application of a particular kind of variation of ζ, where $\delta\zeta \sim (\partial\zeta/\partial\tau)\,\delta\tau$. It follows that

$$\frac{\mathrm{d}k^2}{\mathrm{d}\tau} = -\mathrm{i}\int \zeta^* \frac{\mathrm{d}\zeta}{\mathrm{d}s} \, \mathrm{d}s \Big/ \int\int |\zeta|^2 \, \mathrm{d}A. \tag{24}$$

Since the sign of $\mathrm{i}\int\zeta^*(\mathrm{d}\zeta/\mathrm{d}s)\,\mathrm{d}s$ determines the sense of propagation of the tidal wave, we conclude that when $\mathrm{d}k^2/\mathrm{d}\tau > 0$ the wave advances in the negative direction (negative wave), and vice versa when $\mathrm{d}k^2/\mathrm{d}\tau < 0$.

5. Behaviour of the eigenvalues k^2 for small values of τ

Let us expand ζ in a series of real functions ζ_m with complex coefficients a_m

$$\zeta = \sum_m a_m \zeta_m. \tag{25}$$

Substitution of (25) in (13) gives

$$\delta\left\{ \sum_{m,l} a_m a_l^* \left[\int\int \nabla\zeta_m . \nabla\zeta_l \, \mathrm{d}A - \mathrm{i}\tau \int \zeta_l \frac{\partial\zeta_m}{\partial s} \, \mathrm{d}s - k^2 \int\int \zeta_m \zeta_l \, \mathrm{d}A \right] \right\} = 0. \tag{26}$$

Since the variations δa_l^* are arbitrary, it is necessary that

$$\sum_m a_m \left[\int\int \nabla\zeta_m . \nabla\zeta_l \, \mathrm{d}A - \mathrm{i}\tau \int \zeta_l \frac{\partial\zeta_m}{\partial s} \, \mathrm{d}s - k^2 \int\int \zeta_m \zeta_l \, \mathrm{d}A \right] = 0, \tag{27}$$

for all l. The vanishing of the determinant of the a_m allows us to determine the eigenvalues $k^2(\tau)$ as functions of the parameter τ.

When τ is small we can choose, as a basis, the solutions for the case of no rotation ($\tau = 0$)

$$(\nabla^2 + k_m^2)\,\zeta_m = 0, \quad \partial\zeta_m/\partial n = 0. \tag{28}$$

The ζ_m form an orthonormal set. Using the relation

$$\iint \nabla\zeta_m . \nabla\zeta_l \,\mathrm{d}A = -\iint \zeta_m \nabla^2 \zeta_l \,\mathrm{d}A = k_l^2 \iint \zeta_m \zeta_l \,\mathrm{d}A = k_l^2 \delta_{ml}, \tag{29}$$

in (27) we get

$$\tau \sum_m a_m \beta_{lm} + (k_l^2 - k^2)\, a_l = 0, \tag{30}$$

where

$$\beta_{lm} = -\mathrm{i} \int \zeta_l \frac{\partial \zeta_m}{\partial s}\,\mathrm{d}s. \tag{31}$$

We now expand

$$a_m = a_m^0 + a_m^1 \tau + a_m^2 \tau^2 + \ldots, \tag{32}$$

$$k^2 = c^0 + c^1\tau + c^2\tau^2 + \ldots, \tag{33}$$

substitute in (30) and equate the coefficients of each power of τ to zero. It is then possible to show that in certain cases, which depend on the degeneracy of the eigenfunctions ζ_m in the limit of no ration, c^1 vanishes, while in others it does not. Since a similar analysis was given by Rao (1965, 1966), for the special case of a rectangular basin, we shall only state here the results, which apply generally.

In the case of no degeneracy (singlet), $c^1 = 0$, and

$$k^2 = k_r^2 + \tau^2 \sum_{m \neq r} \frac{|\beta_{mr}|^2}{(k_r^2 - k_m^2)} + \ldots. \tag{34}$$

Since for low values of r, $(k_r^2 - k_m^2) < 0$, it follows that c will be negative, and therefore that $\mathrm{d}k^2/\mathrm{d}\tau < 0$. The wave then propagates in the positive direction.

In the case of a doublet degeneracy for which the associated eigenfunctions have *opposite* symmetry, we get

$$k^2 = k_r^2 \pm \tau\,|\beta_{r,\,r+1}|. \tag{35}$$

Here $c^1 \neq 0$, the wave with the negative slope being positive, and the wave with the positive slope negative.

In the case of a doublet with wave functions of *equal* symmetry, we get $c^1 = 0$.

When τ is large, one can show that there are solutions for which

$$k^2 = k_r^{s^2} + (c^2/\tau^2) + \ldots \quad (\tau \to \infty), \tag{36}$$

where the k_r^s are the eigenvalues of the system

$$(\nabla^2 + k_m^{s^2})\,\zeta_m^s = 0, \tag{37}$$

$$\zeta_m^s = 0, \quad \text{on the boundary.} \tag{38}$$

However, these solutions have no physical significance, since, by (9), they imply that σ is imaginary. These solutions are associated with those modes in which $\sigma = O(\omega)$, as $\omega \to \infty$. In figure 22 they are represented by the branches which cross the $\tau = 1$ line.

6. Tides of the Kelvin-wave type

We shall now discuss a class of tidal oscillations in which the free periods tend to constant values as the rotation ω is increased indefinitely. These tides consist of a Kelvin type wave which travels around the periphery of the basin in the positive direction. With τ increasing and σ remaining finite, the eigenvalues k^2 take on negative values, as seen from (9). Because the functional $D(\zeta)$ in (17) is positive for $\tau < 1$, it follows by (22), that in that region of τ, k^2 cannot take on negative values. It can be shown that, except for the trivial solution $\zeta = c$, the function $k^2(\tau)$ can pass through zero only at the point $\tau = 1$. All the (physical) eigenvalues $k_n^2(\tau)$ must therefore pass through the point $\tau = 1$ when going from positive to negative values. For $k^2 < 0$, we get from (22) that $\mathrm{i}\tau\int\zeta^*(\mathrm{d}\zeta/\mathrm{d}s)\,\mathrm{d}s \geqslant 0$, hence, by (24), $\mathrm{d}k^2/\mathrm{d}\tau < 0$, so that the roots decrease indefinitely with increasing τ.

Let us seek solutions of the wave equation

$$\left(\nabla^2 + \frac{\sigma^2 - 4\omega^2}{gh}\right)\zeta = 0, \tag{39}$$

with the boundary condition

$$\left(\sigma\frac{\partial}{\partial n} - \mathrm{i}2\omega\frac{\partial}{\partial s}\right)\zeta = 0, \tag{40}$$

such that σ remains finite as $\omega \to \infty$. For this purpose we adopt the local system of coordinates (n, s), with the coordinate n having the value zero on the boundary s, and becoming negative in the interior of the basin. Anticipating that the tidal energy will be concentrated near the periphery, we replace n by a boundary-like coordinate η given by

$$\eta = 2\omega n. \tag{41}$$

The leading terms in ω in equations (39) and (40) give

$$\left(\frac{\partial^2}{\partial\eta^2} - \frac{1}{gh}\right)\zeta = 0, \tag{42}$$

$$\left(\sigma\frac{\partial}{\partial\eta} - \mathrm{i}\frac{\partial}{\partial s}\right)\zeta = 0 \quad (\eta = 0), \tag{43}$$

of which the appropriate solution, in the original coordinates, is

$$\zeta = \exp\{[(2\omega n - \mathrm{i}\sigma s)/\sqrt{(gh)}] + \mathrm{i}\sigma t\}. \tag{44}$$

The eigenfrequency σ must be such that as s increases and we make a complete turn around the periphery of the basin, the factor $\exp\{\mathrm{i}\sigma s/\sqrt{(gh)}\}$ remains single-valued. If p denotes the perimeter of the basin, we must have

$$\sigma_n = 2\pi n\sqrt{(gh)}/p. \tag{45}$$

These characteristic frequencies are determined therefore by the perimeter p and the depth h, independently of the speed of rotation ω, as long as the latter is large (in comparison with σ). Equation (44) shows that the tidal wave travels in the positive direction, and with a speed $\sqrt{(gh)}$ characteristic of the Kelvin wave. The amplitude decreases exponentially as we recede from the boundary into the interior in the direction of the normal according to $\exp\{2\omega n/\sqrt{(gh)}\}$, which is characteristic of the Kelvin wave.

7. Solution for the tides in a rotating basin by method A

In method A we attempt to solve for the tidal oscillations by expanding ζ, in the first instance, in terms of the eigenfunctions for the case of no rotation

$$\zeta = \sum_m a_m \zeta_m, \quad (\nabla^2 + k_m^2)\,\zeta = 0, \tag{46}$$

which satisfy the condition $\partial\zeta_m/\partial n = 0$ on the boundary. By (10), this expansion would be expected to converge well for small values of τ. As was shown in § 5, substitution of (46) into the variational equation (13) leads to the system (30) for the determination of the coefficients a_m (complex), which for unnormalized eigenfunctions ζ_m takes on the form

$$\tau \sum_m a_m \beta_{lm} + (k_l^2 - k^2)\, N_l^2\, a_l = 0, \tag{47}$$

$$N_l^2 = \int\int \zeta_l^2 \,\mathrm{d}A, \quad \beta_{lm} = -\mathrm{i} \int \zeta_l \frac{\partial \zeta_m}{\partial s}\,\mathrm{d}s. \tag{48}$$

For a rectangle defined by $$0 \leqslant x \leqslant a, \quad 0 \leqslant y \leqslant b, \tag{49}$$

the eigenfunctions are $$\zeta_{mn} = \cos\frac{m\pi x}{a}\cos\frac{n\pi y}{b}, \tag{50}$$

$$k_{mn}^2 = \frac{m^2\pi^2}{a^2} + \frac{n^2\pi^2}{b^2}. \tag{51}$$

The integral on the boundary becomes

$$\int \zeta_{kl} \frac{\partial \zeta_{mn}}{\partial s}\,\mathrm{d}s = 4p(m,k)\,p(n,l)\left[\frac{n^2}{m^2-l^2} - \frac{m^2}{m^2-k^2}\right], \tag{52}$$

where $$p(m,k) = m+k \pmod 2 = 1 \quad ((m+k) \text{ odd}) \tag{53}$$
$$= 0 \quad ((m+k) \text{ even}).$$

With $$N_{kl}^2 = \int\int \zeta_{kl}^2 \mathrm{d}A = \tfrac{1}{4}ab(1+\delta_{0k})\,(1+\delta_{0l}), \tag{54}$$

$$a_{mn} \equiv \mathrm{i}^m \alpha_{mn}, \tag{55}$$

equation (47) becomes

$$\tau \sum_{m,n} \alpha_{mn}\, \mathrm{i}^{m-k-1} 4p(m,k)\,p(n,l)\left[\frac{n^2}{n^2-l^2} - \frac{m^2}{m^2-k^2}\right] + \alpha_{kl}(k_{kl}^2 - k^2)\,\tfrac{1}{4}ab(1+\delta_{0k})\,(1+\delta_{0l}) = 0. \tag{56}$$

Here k and l take on integral values, with zero omitted. Since the coefficient of α_{mn} is different from zero only if $(m-k)$ is odd, the coefficients in (56) are real.

The solutions separate into two independent systems of different symmetry. The even solutions include the ζ_{mn} for which m and n have the same parity. These solutions ζ_e are symmetrical with respect to the centre of the rectangle

$$\zeta_e(z^1) = \zeta_e(z), \tag{57}$$

where z^1 is the reflexion of the point z through the centre. In the odd solutions ζ_0, the

indices m and n have different parity, and they are antisymmetrical with respect to the origin

$$\zeta_0(z^1) = -\zeta_0(z). \tag{58}$$

The system of equations (56) is of the form

$$(\tau A - \lambda D)\, X = 0, \tag{59}$$

where the eigenvalues λ are to be found as functions of the parameter τ. The matrix A is symmetrical, and D is positive diagonal, showing the advantage of adopting the parameters k^2 and τ in place of σ and ω.

We have applied method A to the tidal problems in a square basin, with $a = b = 2$. The convergence was good only for values of $\tau < 1$. In order to improve the convergence for larger values of τ we added to our base (50) the system

$$\zeta^s_{mn} = \sin\frac{m\pi x}{a}\sin\frac{n\pi y}{b}, \tag{60}$$

$$(k^s_{mn})^2 = \pi^2\left(\frac{m^2}{a^2}+\frac{n^2}{b^2}\right), \tag{61}$$

which satisfy the condition $\zeta^s_{mn} = 0$ on the boundary. Even so, the convergence was slow, and as many as 50 terms were required to cover the range of τ up to 2.

8. Method B

In this method we use for ζ in the variational equation (13) an expansion in terms of a set of functions ζ_n which satisfies the equation

$$(\nabla^2 + k^2)\,\zeta_n = 0, \tag{62}$$

and which is complete on the boundary. No restrictions are put on the ζ_n by boundary conditions, so that k^2 enters as a continuous parameter. The method is due to Trefftz (Collatz 1965; see also Davis & Rabinowitz 1961). By partial integration and the use of (62), the surface integrals in (13) drop out, and we are left with only the line-integral taken along the boundary s

$$\delta\left\{\int \zeta^*\left(\frac{\partial}{\partial n} - \mathrm{i}\tau\frac{\partial}{\partial s}\right)\zeta\,\mathrm{d}s\right\} = 0. \tag{63}$$

In (63) the parameter k^2 enters implicitly in the functions ζ, and the variation yields the discrete eigenvalues τ_n for a given value of k^2. Since the set ζ_n is complete on a line, and not on an area, it is one-dimensional, rather than two-dimensional.

Let us put in (63) the expansion

$$\zeta = \sum_n (\alpha_n \zeta_n + \mathrm{i}\beta_n \eta_n), \tag{64}$$

where η_n also satisfies (62), and α_n, β_n, ζ_n and η_n are all real. We get

$$\sum_n \int \{\alpha_n[\zeta_n D\zeta_l + \zeta_l D\zeta_n] + \mathrm{i}\beta_n[-\eta_n D\zeta_l + \zeta_l D\eta_n]\}\,\mathrm{d}s = 0, \tag{65}$$

$$\sum_n \int \{\mathrm{i}\alpha_n[\zeta_n D\eta_l - \eta_l D\zeta_n] + \beta_n[\eta_n D\eta_l + \eta_l D\eta_n]\}\,\mathrm{d}s = 0, \tag{66}$$

PHILOSOPHICAL TRANSACTIONS OF THE ROYAL SOCIETY A MATHEMATICAL, PHYSICAL & ENGINEERING SCIENCES

where
$$D\zeta \equiv \left(\frac{\partial}{\partial n} - i\tau \frac{\partial}{\partial s}\right)\zeta. \tag{67}$$

Since for any pair of functions ω_1 and ω_2 which satisfy the wave equation (62) we have

$$\int \left(\omega_1 \frac{\partial \omega_2}{\partial s} + \omega_2 \frac{\partial \omega_1}{\partial s}\right) ds = 0, \tag{68}$$

$$\int \left(\omega_1 \frac{\partial \omega_2}{\partial n} - \omega_2 \frac{\partial \omega_1}{\partial n}\right) ds = 0, \tag{69}$$

equations (65) and (66) reduce to

$$\sum_n \int \left[\alpha_n \zeta_l \frac{\partial \zeta_n}{\partial n} + \tau \beta_n \zeta_l \frac{\partial \eta_n}{\partial s}\right] ds = 0, \tag{70}$$

$$\sum_n \int \left[\tau \alpha_n \zeta_n \frac{\partial \eta_l}{\partial s} + \beta_n \eta_l \frac{\partial \eta_n}{\partial n}\right] ds = 0. \tag{71}$$

These represent simultaneous equations for the determination of the coefficients α_n and β_n, and the vanishing of the determinant of these equations yields the eigenvalues τ_n for a given k^2.

9. Free tidal oscillations in a rotating flat rectangular basin

Method B, as given by equations (64), (70) and (71), can be applied directly to the case of a rectangular basin. Let the basin be defined in $|x| \leqslant a$, $|y| \leqslant b$. For the symmetrical waves we put

$$\zeta = \sum_n [\alpha_n \cos \lambda_n x \cos \mu_n y + i\beta_n \sin \lambda_n x (\sin \mu_n y/\mu_n)], \tag{72}$$

where $\lambda_n = (\pi n/2a)$, and

$$\mu_n = (k^2 - \lambda_n^2)^{\frac{1}{2}}, \tag{73}$$

so as to satisfy the wave equation (62). With (72), equations (70) and (71) take on the form

$$\sum_n \{\alpha_n(-u_{kn}\mu_n \cos \mu_k b \sin \mu_n b - w_{kn}\lambda_n \sin \lambda_n a \cos \lambda_k a) + \tau\beta_n[-u_{kn}\lambda_n \cos \mu_k b (\sin \mu_n b/\mu_n) + w_{kn} \sin \lambda_n a \cos \lambda_k a]\} = 0 \quad (k = 0, 1, 2, \ldots), \tag{74}$$

$$\sum_n \{\tau\alpha_n[-u_{kn}\lambda_k \cos \mu_n b (\sin \mu_k b/\mu_k) + w_{kn} \sin \lambda_k a \cos \lambda_n a] + \beta_n[v_{kn} \cos \mu_n b (\sin \mu_k b/\mu_k) + (t_{kn}\lambda_n/\mu_k\mu_n) \sin \lambda_k a \cos \lambda_n a]\} = 0 \quad (k = 1, 2, \ldots). \tag{75}$$

Here
$$u_{kn} = \int_{-a}^{a} \cos \lambda_k x \cos \lambda_n x \, dx, \quad w_{kn} = \int_{-b}^{b} \cos \mu_k y \cos \mu_n y \, dy, \tag{76}$$

$$v_{kn} = \int_{-a}^{a} \sin \lambda_k x \sin \lambda_n x \, dx, \quad t_{kn} = \int_{-b}^{b} \sin \mu_k y \sin \mu_n y \, dy. \tag{77}$$

In the case of antisymmetrical waves we put

$$\zeta = \sum_n [\alpha_n \cos \lambda_n x (\sin \mu_n y/\mu_n) + i\beta_n \sin \lambda_n x \cos \mu_n y], \tag{78}$$

where λ_n and μ_n are as defined before. Equations (70) and (71) now become

$$\sum_n \{\alpha_n[u_{kn}\cos\mu_n b(\sin\mu_k b/\mu_k) - \lambda_n \sin\lambda_n a\cos\lambda_k a(t_{kn}/\mu_k\mu_n)] + \tau\beta_n[-u_{kn}\lambda_n\cos\mu_n b(\sin\mu_k b/\mu_k) - \sin\lambda_n a\cos\lambda_k a(\mu_n t_{kn}/\mu_k)]\} = 0 \quad (k=0,1,2,\ldots) \tag{79}$$

$$\sum_n \{\tau\alpha_n[-u_{kn}\lambda_k\cos\mu_k b(\sin\mu_n b/\mu_n) - \sin\lambda_k a\cos\lambda_n a(\mu_k t_{kn}/\mu_n)] + \beta_n[-v_{kn}\mu_n\sin\mu_n b\cos\mu_k b + w_{kn}\lambda_n\sin\lambda_k a\cos\lambda_n a]\} = 0 \quad (k=1,2,\ldots). \tag{80}$$

The integrals in (76) and (77) can be readily evaluated, so that the coefficients in the equations (74) and (75), as well as in (79) and (80), can be evaluated with as high an accuracy as is needed.

We have treated the case of a square basin and have solved for the eigenvalues and eigenfunctions of the determinant of these equations. The results are shown in figures 22 to 31. The convergence by method B was good, with a determinant of order 12 yielding an accuracy which could only be achieved by a determinant of order 50 when method A, described in § 7, was used.

10. Free tidal oscillations in a rotating flat basin of the shape of a circular sector

Referring to figure 1, let the basin be bounded by

$$-\frac{\pi}{2\mu} \leqslant \theta \leqslant \frac{\pi}{2\mu} \quad (0 \leqslant r \leqslant 1), \tag{81}$$

where μ can take on any value greater than $\frac{1}{2}$. In a cylindrical system of coordinates (r,θ), the solutions of the wave equation (62) which have the appropriate singularity as the apex of a wedge are (Fox 1961)

$$\zeta = \sum_{n=0}^{\infty} J_{\mu n}(kr)\,[\alpha_n\cos\mu n\theta + \mathrm{i}\beta_n\sin\mu n\theta]. \tag{82}$$

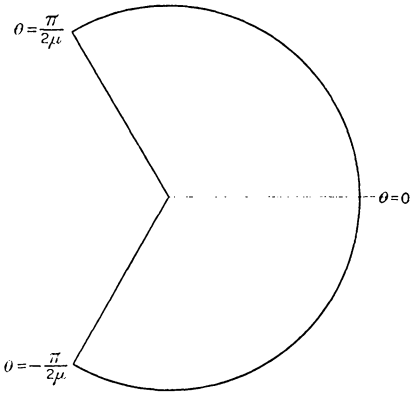

Figure 1. Tidal basin of circular sector of total angular width π/μ.

Here π/μ designates the angular opening of the circular segment according to (81). Putting

$$a_{ln} = \int_0^k J_{\mu l}(z)J_{\mu n}(z)\frac{\mathrm{d}z}{z}, \quad b_{ln} = \int_0^k \dot{J}_{\mu l}(z)\,J_{\mu n}(z)\,\mathrm{d}z, \tag{83}$$

$$c_{ln} = \int_0^{\pi/2\mu} \cos\mu l\theta\cos\mu n\theta\,\mathrm{d}\theta, \quad d_{ln} = \int_0^{\pi/2\mu} \sin\mu l\theta\sin\mu n\theta\,\mathrm{d}\theta, \tag{84}$$

PHILOSOPHICAL TRANSACTIONS OF THE ROYAL SOCIETY A MATHEMATICAL, PHYSICAL & ENGINEERING SCIENCES

the system of equations (70) and (71) in method B, with ζ given by (82), becomes

$$\sum_n \{\alpha_n[-\mu n a_{ln} \sin \tfrac{1}{2}n\pi \cos \tfrac{1}{2}l\pi + k c_{ln} J_{\mu l}(k) \dot{J}_{\mu n}(k)] + \tau\beta_n[c_{ln}\mu n J_{\mu l}(k) J_{\mu n}(k) - b_{nl} \sin \tfrac{1}{2}l\pi \cos \tfrac{1}{2}n\pi]\} = 0 \quad (l = 0, 1, 2, \ldots) \quad (85)$$

$$\sum_n \{\tau\alpha_n[c_{ln}\mu l J_{\mu l}(k) J_{\mu n}(k) - b_{ln} \sin \tfrac{1}{2}n\pi \cos \tfrac{1}{2}l\pi] + \beta_n[a_{ln}\mu n \sin \tfrac{1}{2}l\pi \cos \tfrac{1}{2}n\pi + k d_{ln} J_{\mu l}(k) \dot{J}_{\mu n}(k)]\} = 0 \quad (l = 1, 2, \ldots) \quad (86)$$

In evaluating the coefficients in the system of equations (85) and (86), the trigonometric integrals c_{ln} and d_{ln} of (84) are obtained in closed form. For the Bessel integrals a_{ln} and b_{ln} defined in (83), we developed the integrands into power series and the integration was carried out to high accuracy.

In this configuration, the only symmetry that exists for the tide is with respect to the axis $\theta = 0$, for which we have

$$\zeta(r, -\theta) = \zeta^*(r, \theta). \quad (87)$$

Equations (85) and (86) were solved for circular basins having total angular openings of $\frac{1}{2}\pi$, π and $\frac{3}{2}\pi$. The results are shown in figures 2 to 21.

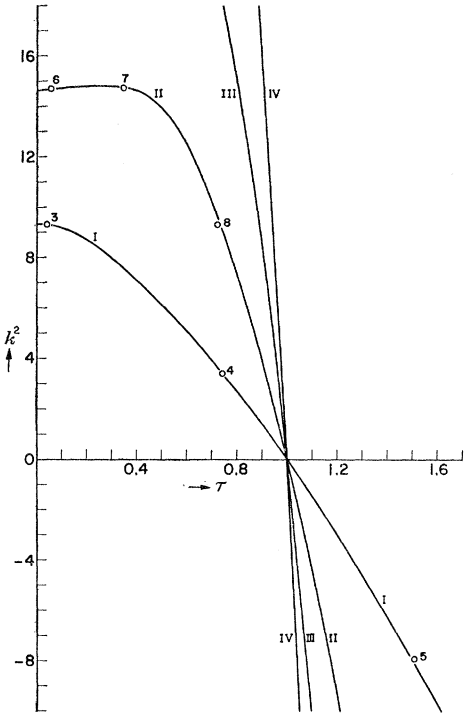

FIGURE 2

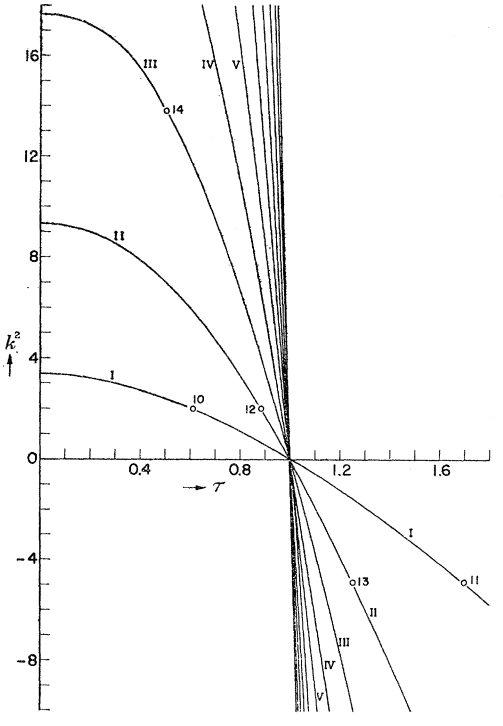

FIGURE 9

FIGURE 2. Dependence of the frequency parameter k^2 on the rotation parameter τ for tidal oscillations in a 90° circular sector. $k^2 = (\sigma^2 - 4\omega^2)/gh$, $\tau = 2\omega/\sigma$. σ is the frequency, ω the angular rotation of the basin, h the depth of liquid. Numbers on graphs give the figure numbers where the respective tidal flows are shown.

FIGURE 9. Dependence of the frequency parameter k^2 on the rotation parameter τ for tidal oscillations in a semicircular sector. $k^2 = (\sigma^2 - 4\omega^2)/gh$, $\tau = 2\omega/\sigma$. σ is the frequency, ω the angular rotation of the basin, h the depth of liquid. Numbers on graphs give the figure numbers where the respective tidal flows are shown.

PHILOSOPHICAL TRANSACTIONS OF THE ROYAL SOCIETY A MATHEMATICAL, PHYSICAL & ENGINEERING SCIENCES

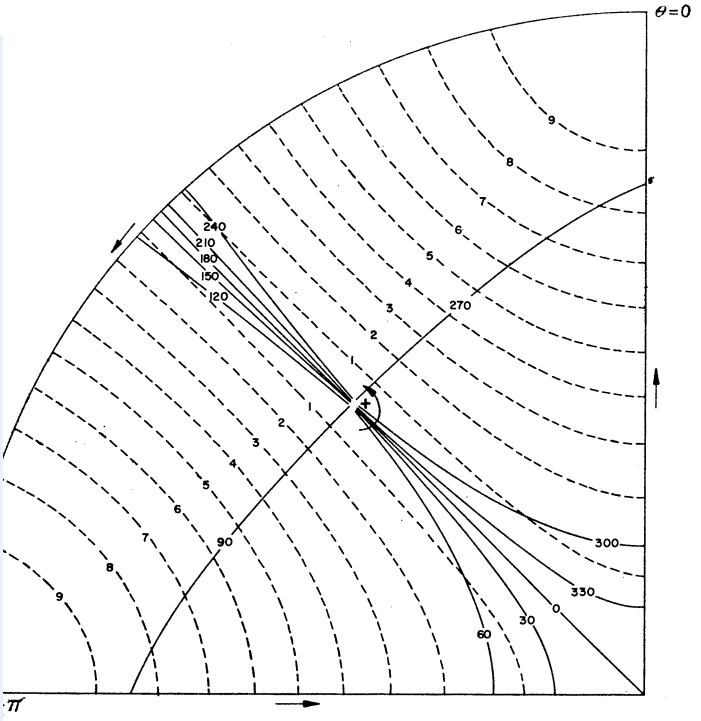

$\mu = 2,\ k^2 = 9{\cdot}3,\ \tau = 0{\cdot}041$

FIGURE 3

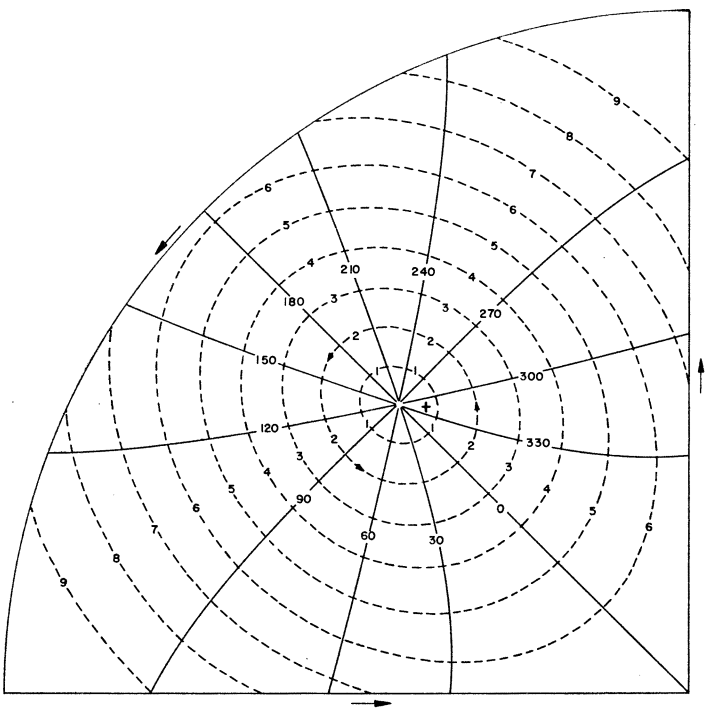

$\mu = 2,\ k^2 = 3{\cdot}4,\ \tau = 0{\cdot}741$

FIGURE 4

FIGURE 3. Free tidal oscillations in a 90° circular sector. $\tau = 2\omega/\sigma$, $k^2 = (\sigma^2 - 4\omega^2)/gh$. — co-tidal lines, – – – co-range lines. The angular opening of the basin is π/μ. First mode at slow rotation. Positive wave.

FIGURE 4. Free tidal oscillations in a 90° circular sector. $\tau = 2\omega/\sigma$, $k^2 = (\sigma^2 - 4\omega^2)/gh$. — co-tidal lines, – – – co-range lines. First mode at moderate rotation. Positive wave.

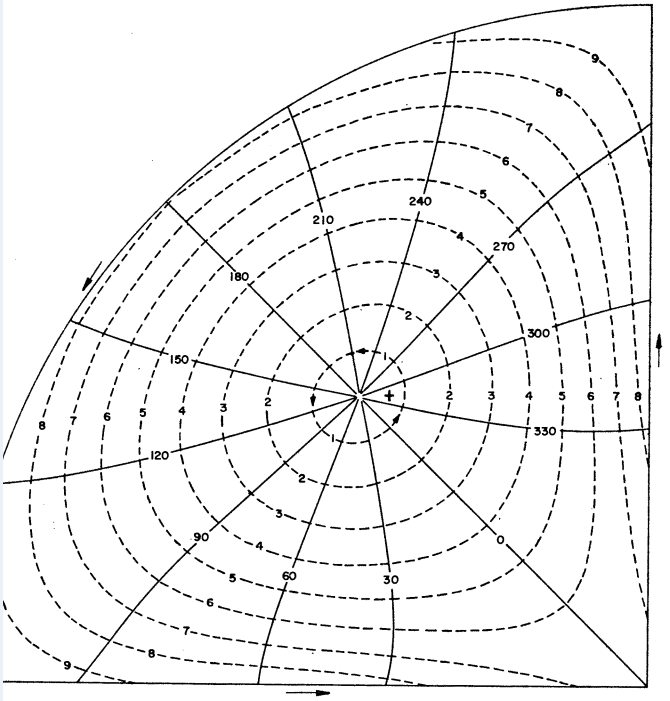

$\mu = 2,\ k^2 = -7{\cdot}9,\ \tau = 1{\cdot}511$

FIGURE 5

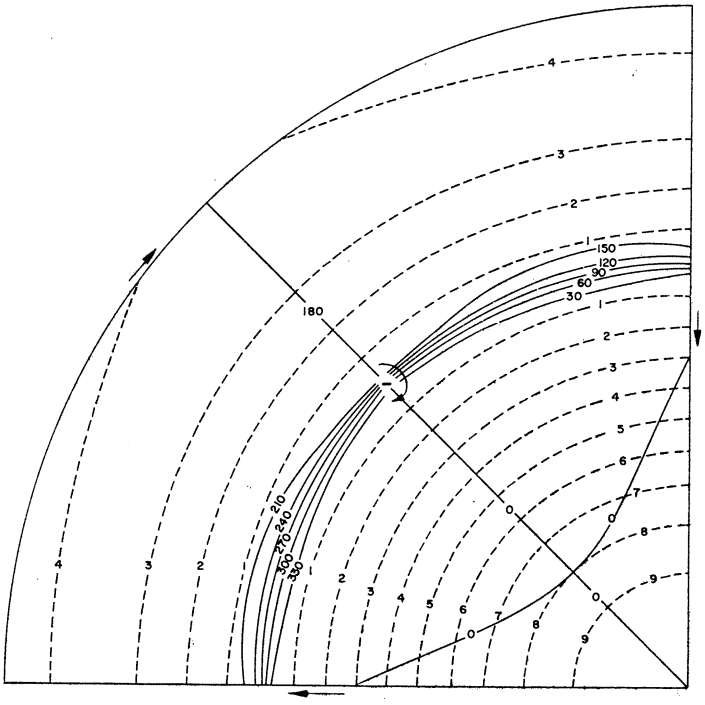

$\mu = 2,\ k^2 = 14{\cdot}7,\ \tau = 0{\cdot}061$

FIGURE 6

FIGURE 5. First mode, fast rotation. Approach to a Kelvin-type wave. Positive wave.

FIGURE 6. Second mode, slow rotation. Negative wave.

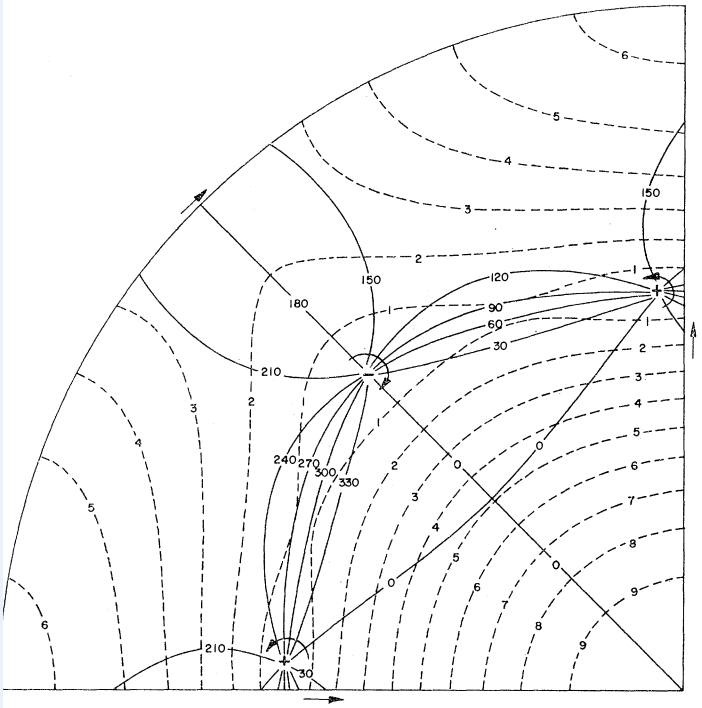

FIGURE 7

$\mu = 2$, $k^2 = 14{\cdot}7$, $\tau = 0{\cdot}349$

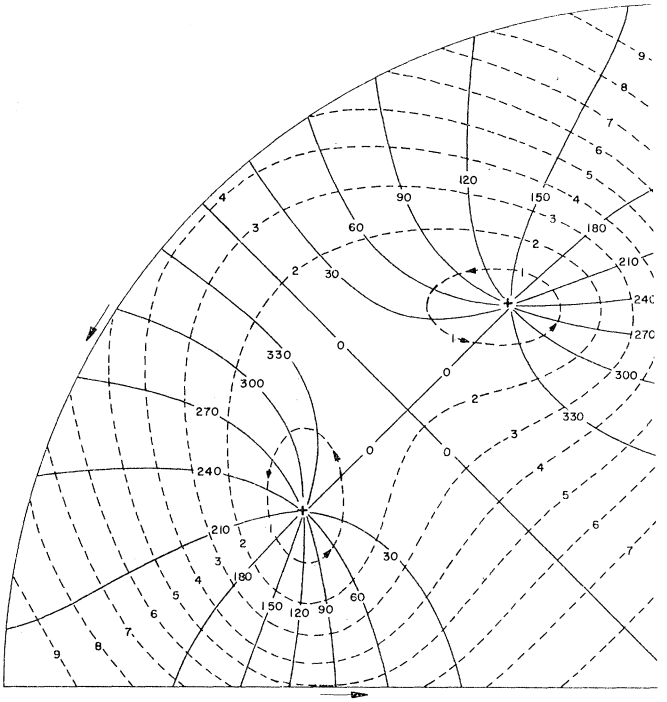

FIGURE 8

$\mu = 2$, $k^2 = 9{\cdot}3$, $\tau = 0{\cdot}724$

FIGURE 7. As the rotation is increased above that in figure 6, there appear two positive amphidromic systems near the radial coastlines, while the amphidromic system in the interior is still negative. Mixed wave.

FIGURE 8. As the rotation is further increased beyond that of figure 7, the original negative amphidromic system disappears altogether. Positive wave.

11. Discussion of results

The frequency characteristics for the first 4 modes of the tidal oscillations in a flat basin of the form of a 90° circular sector are shown in figure 2. The graphs give the dependence of the frequency parameter $k^2 = (\sigma^2 - 4\omega^2)/gh$ on the rotation parameter $\tau = 2\omega/\sigma$. All curves pass through the point $\tau = 1$ $(2\omega = \sigma)$, and for higher rotations ω, k^2 is negative. Figure 3 shows the tidal pattern when the rotation of the basin is relatively small $(\tau = 0{\cdot}041)$. The solid lines give the locus of points where the phase ϕ appearing in the factor

$$\zeta = r \exp \mathrm{i}(\sigma t + \phi)$$

is constant and has the value indicated. The tidal wave advances in a direction of *decreasing* ϕ. We call a tidal wave positive if it advances in the direction of rotation, which is counterclockwise. The arrows show the direction of propagation of the wave on the coastline. The tide-height is given on a relative scale, in which the maximum amplitude has the value of 10. An *amphidromic point* is a point in which the tide height is zero, and from which radiate outwards the co-tidal lines. In the case of no rotation, the fluid to the right of the $\theta = \frac{1}{4}\pi$ line (viewed from the centre) would swing in one phase, while the fluid to the left would swing all in the opposite phase. In the presence of slow rotation, the change of phase by

180° takes place over a narrow zone around the $\theta = \frac{1}{4}\pi$ radius, rather than abruptly on the radius.

As the rotation speed 2ω increases and becomes comparable to the frequency σ, we see in figure 4 that the phase transition becomes distributed nearly uniformly in angle around the amphidromic point. The curvature of the co-range lines has become convex, except near the origin. At larger rotation, shown in figure 5, the tide height assumes a nearly uniform high value on the coast, especially on the curved part, where it is everywhere greater than 8. This indicates the transition to a Kelvin-type wave, where the tidal amplitude is a maximum on the coastline and decreases exponentially in the direction of the normal to the coastline, as given by equation (44).

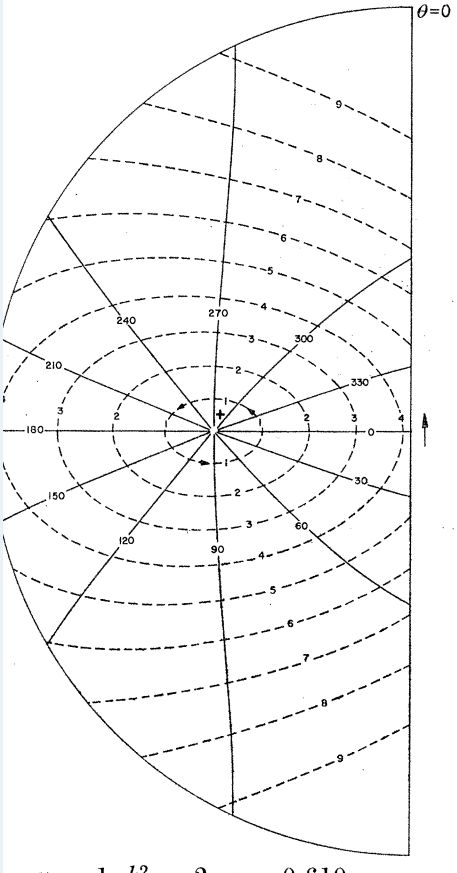

$\mu = 1, k^2 = 2, \tau = 0{\cdot}610$

FIGURE 10

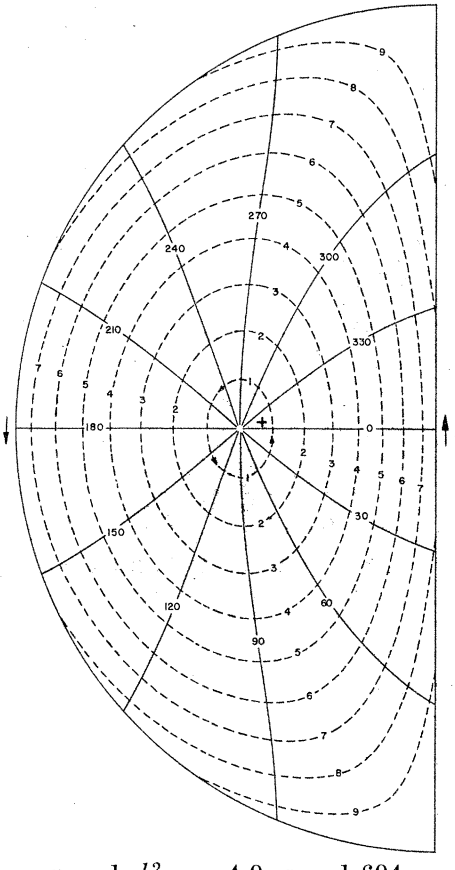

$\mu = 1, k^2 = -4{\cdot}9, \tau = 1{\cdot}694$

FIGURE 11

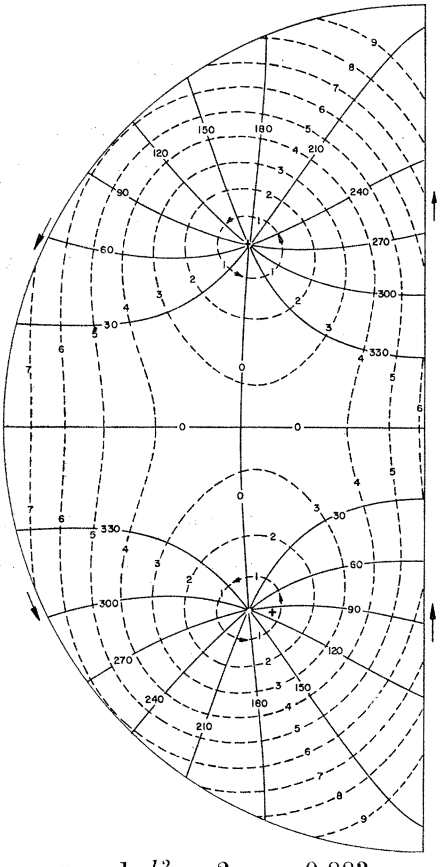

$\mu = 1, k^2 = 2, \tau = 0{\cdot}883$

FIGURE 12

FIGURE 10. Free tidal oscillations in a semicircular basin. $\tau = 2\omega/\sigma$, $k^2 = (\sigma^2 - 4\omega^2)/gh$, — co-tidal lines, – – – co-range lines. First mode. Moderate rotation. Positive wave.

FIGURE 11. Free tidal oscillations in a semicircular basin at high rotation. Approach to Kelvin-type wave. First mode, positive wave.

FIGURE 12. Free tidal oscillations in a semicircular basin. Second mode at moderate rotation. Positive wave.

We note that in the first mode, the total change of phase around the periphery is 2π, and that the wave is everywhere positive. The latter feature is in conformity with the curve $k^2(\tau)$ for the first mode in figure 2, which has a negative slope everywhere. The curve $k^2(\tau)$ for the second mode, shown in figure 2, is different, in that for small values of τ we have

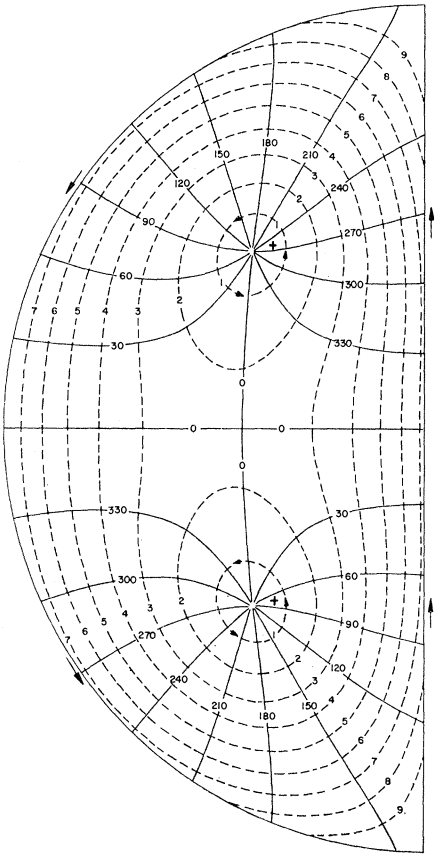

$\mu = 1,\ k^2 = -4{\cdot}9,\ \tau = 1{\cdot}252$

FIGURE 13

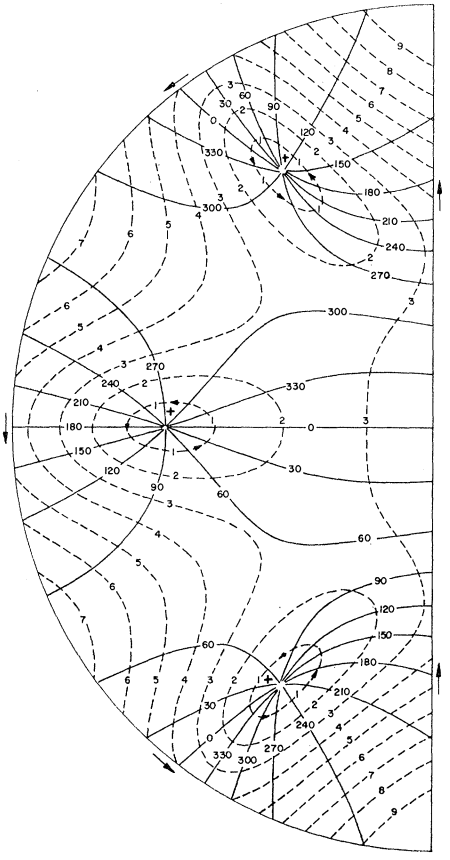

$\mu = 1,\ k^2 = 13{\cdot}8,\ \tau = 0{\cdot}507$

FIGURE 14

FIGURE 13. Second mode at high rotation. Approach to Kelvin regime. Positive wave.

FIGURE 14. Third mode, at moderate rotation. Positive wave.

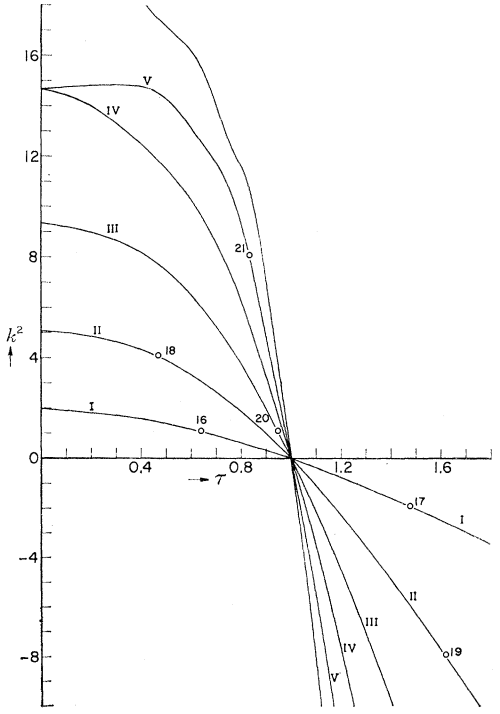

FIGURE 15. Dependence of the frequency parameter k^2 on the rotation parameter τ for tidal oscillations in a 270° circular sector. $k^2 = (\sigma^2 - 4\omega^2)/gh$, $\tau = 2\omega/\sigma$. σ is the frequency, ω the angular rotation of the basin, h the depth of liquid. Numbers on graphs give the figure numbers where the respective tidal flows are shown.

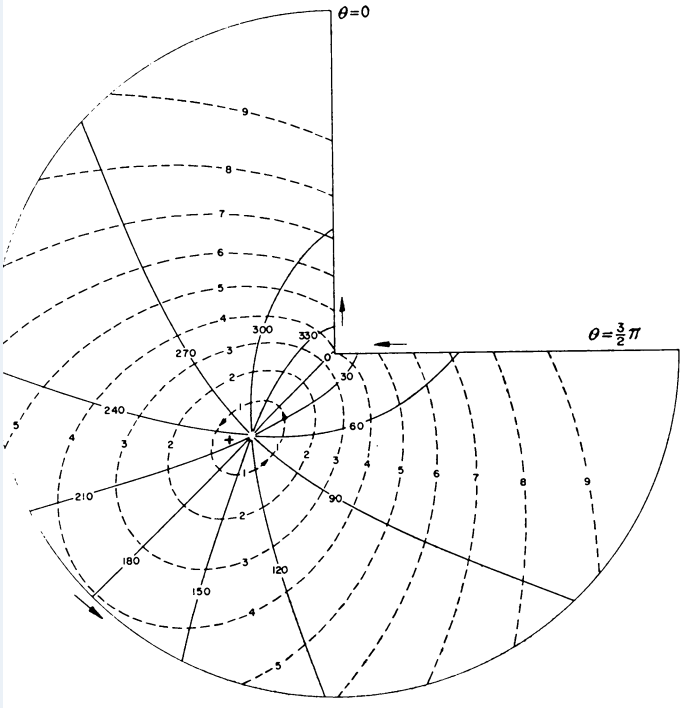

$\mu = \frac{2}{3}$, $k^2 = 1{\cdot}1$, $\tau = 0{\cdot}638$

FIGURE 16

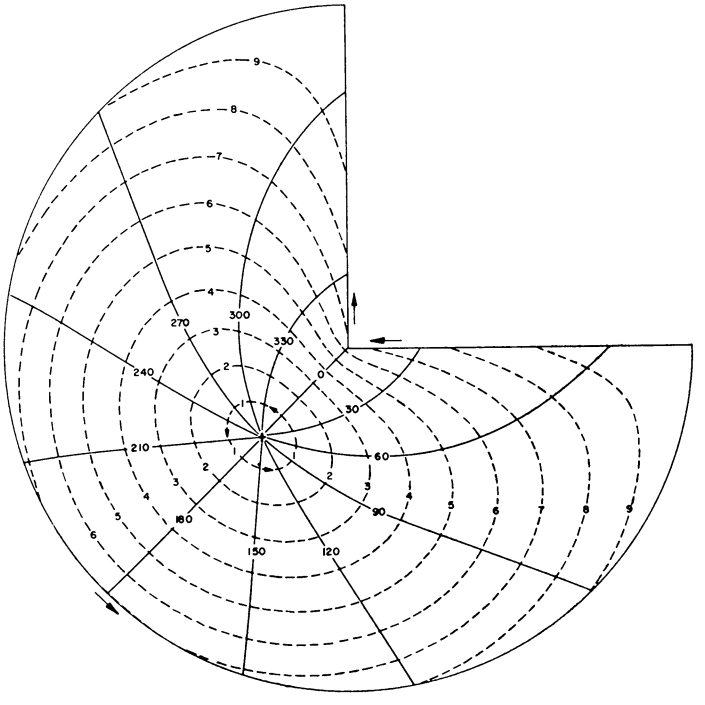

$\mu = \frac{2}{3}$, $k^2 = -1{\cdot}9$, $\tau = 1{\cdot}475$

FIGURE 17

FIGURE 16. Free tidal oscillations in a 270° circular sector. $\tau = 2\omega/\sigma$, $k^2 = (\sigma^2 - 4\omega^2)/gh$, — co-tidal lines, – – – co-range lines. First mode at moderate rotation. Positive wave.

FIGURE 17. First mode at moderately large rotation. Kelvin regime not yet established. Positive wave.

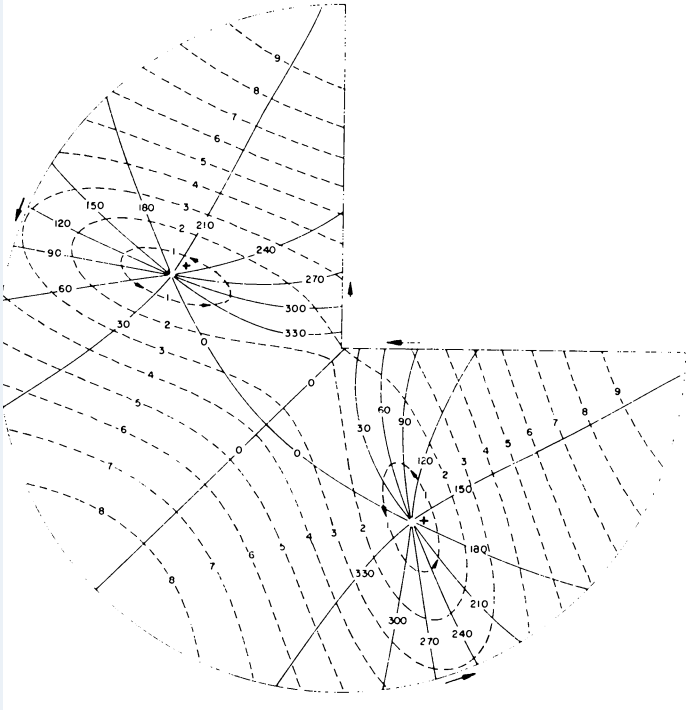

$\mu = \frac{2}{3}$, $k^2 = 4{\cdot}1$, $\tau = 0{\cdot}467$

FIGURE 18

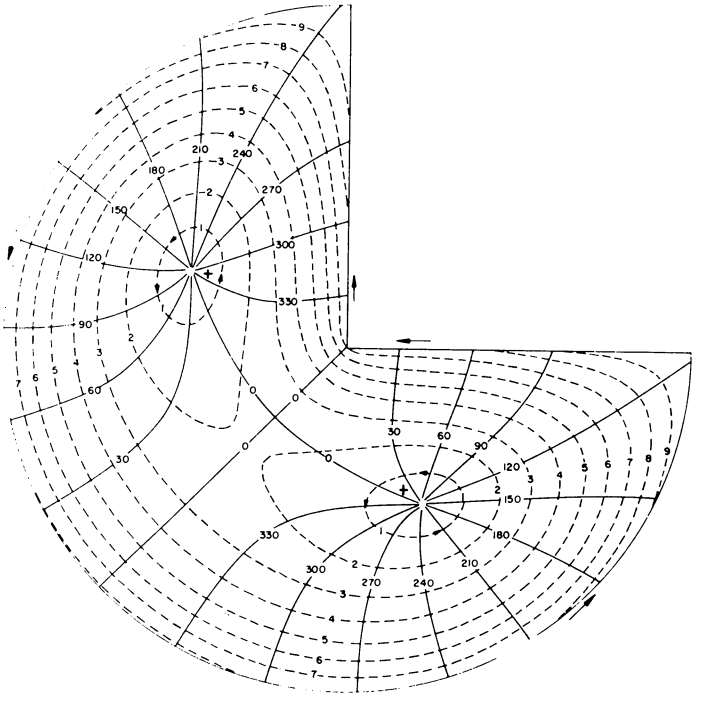

$\mu = \frac{2}{3}$, $k^2 = -7{\cdot}9$, $\tau = 1{\cdot}619$

FIGURE 19

FIGURE 18. Second mode at slow rotation. Positive wave.

FIGURE 19. Second mode at large rotation. Approach to Kelvin regime. Positive wave.

$dk^2/d\tau > 0$. This implies, according to the discussion in § 4, that for small rotation the tidal wave is negative, and that the tide advances along the coast in a direction opposite to that of the rotation of the basin. This is illustrated in figure 6. As τ is increased in curve II and we pass the maximum, we see in figure 7 that the change of sign of $dk^2/d\tau$ manifests itself by the appearance of two *positive* amphidromic points near the radial coastlines, which the main amphidromic system in the centre is still negative. The tidal wave is now of a mixed character, advancing in the negative direction along the curved portion of the coastline, and in the positive direction along the radial portions. As the rotation is further increased, the negative amphidromic system disappears altogether, and there remain only the two positive amphidromic systems, as shown in figure 8. The total change of phase around the periphery of the basin is now 4π.

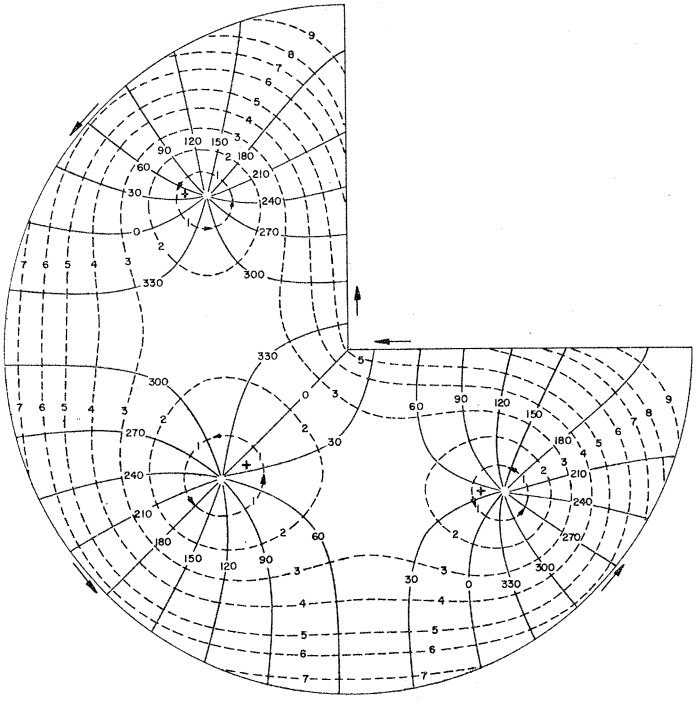

$\mu = \frac{2}{3}$, $k^2 = 1{\cdot}1$, $\tau = 0{\cdot}946$

FIGURE 20

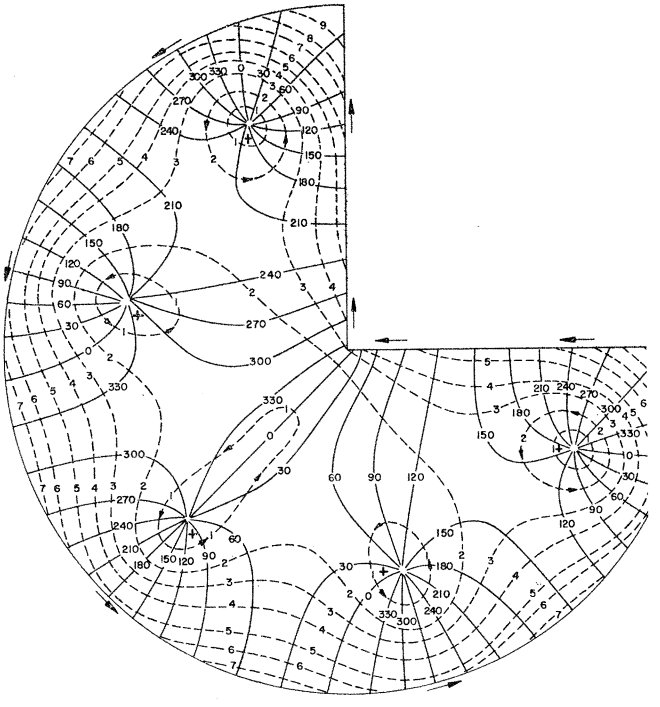

$\mu = \frac{2}{3}$, $k^2 = 8{\cdot}1$, $\tau = 0{\cdot}830$

FIGURE 21

FIGURE 20. Third mode at moderate rotation. Signs of Kelvin regime. Positive wave.

FIGURE 21. Fifth mode at moderate rotation. Approach to Kelvin regime. Positive wave.

The frequency characteristics for a semicircular basin are shown in figure 9 for the first 10 modes (see Proudman 1928). In the first mode and at moderate rotation, shown in figure 10, the central co-range lines are elliptical, with the long axis oriented along the radius of $\theta = \frac{1}{2}\pi$. As $\tau \to 0$ these ellipses collapse to the radius. At moderately large rotation, shown in figure 11, the co-range lines have elliptical shape but conform now more to the coastline. The high and uniform amplitudes along the coastline indicate the approach to a Kelvin regime. The second mode is shown in figures 12 and 13, with the latter exhibiting the crowding of the tidal energy away from the interior towards the coastline as the rotation increases. Figure 14 shows the third mode at moderate rotation. All the waves shown for the

semicircular basin are positive, and the phase changes by $2\pi n$ as we go around the circumference, n denoting the order of the mode.

The frequency characteristics for a flat basin of the form of a 270° circular basin are shown in figure 15. At moderate rotation, the first mode shown in figure 16 exhibits co-range lines of elliptical shape oriented along the radius of $\theta = \frac{3}{4}\pi$, which is the nodal line at no rotation. At higher rotation speeds, shown in figure 17, the co-range lines begin to conform in shape to the coastline, as required in the Kelvin regime. The second mode is illustrated in figures 18 and 19, with the latter quite Kelvin-like. An example of the third mode is shown in figure 20, and of the fifth mode in figure 21. All the cases shown have positive waves along the coastline.

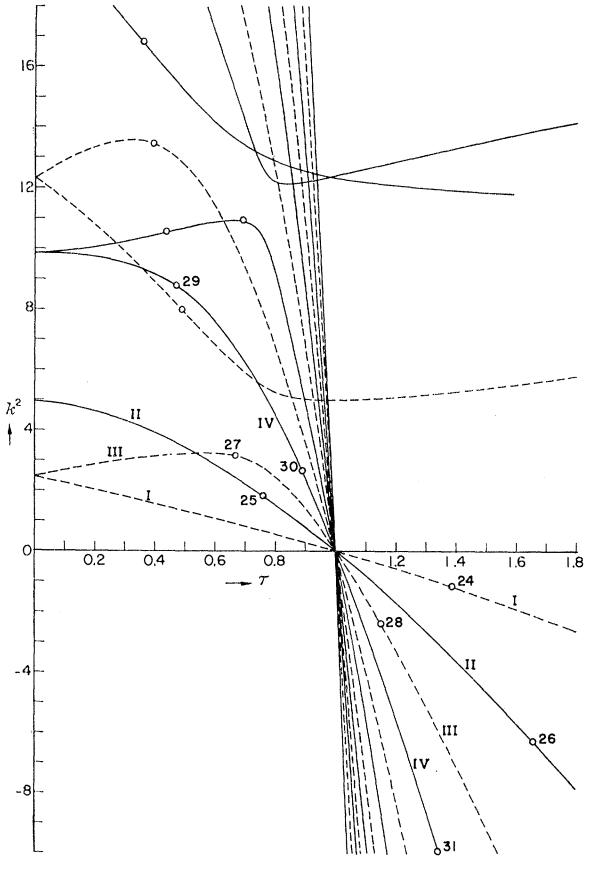

FIGURE 22

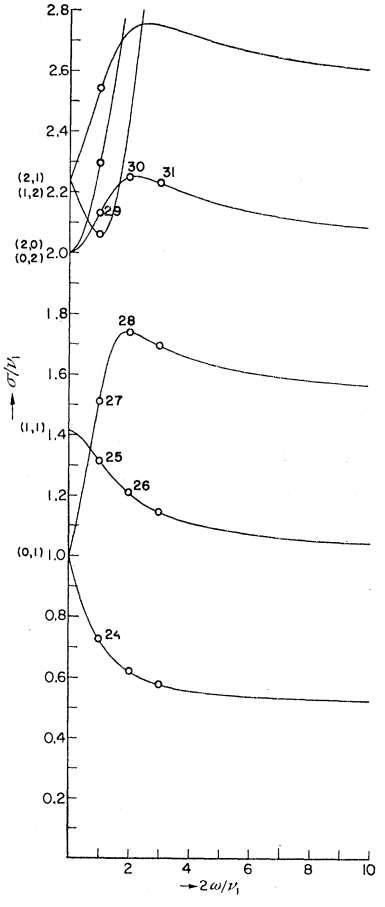

FIGURE 23

FIGURE 22. Frequency characteristics of tidal oscillations in a rotating square flat basin. $\tau = 2\omega/\sigma$, $k^2 = (\sigma^2 - 4\omega^2)/gh$. — symmetrical oscillations, – – – antisymmetrical oscillations.

FIGURE 23. The frequency σ as a function of the angular speed of rotation ω for the tidal oscillations in a square flat rotating basin. $\nu_1 = \frac{1}{2}\pi$ is the lowest frequency for the square basin in the case of no rotation.

We have applied the analysis given in § 9 to the tidal oscillations of a rotating flat square basin. The dependence of frequency parameter $k^2 = (\sigma^2 - 4\omega^2)/gh$ on the speed of rotation parameter $\tau = 2\omega/\sigma$ is shown in figure 22. Here, the continuous lines refer to symmetrical oscillations (equations (74) and (75)), and the dashed lines to antisymmetrical oscillations (equations (79) and (80)). Most of the roots are double, with one curve $k^2(\tau)$ increasing

PHILOSOPHICAL TRANSACTIONS OF THE ROYAL SOCIETY A MATHEMATICAL, PHYSICAL & ENGINEERING SCIENCES

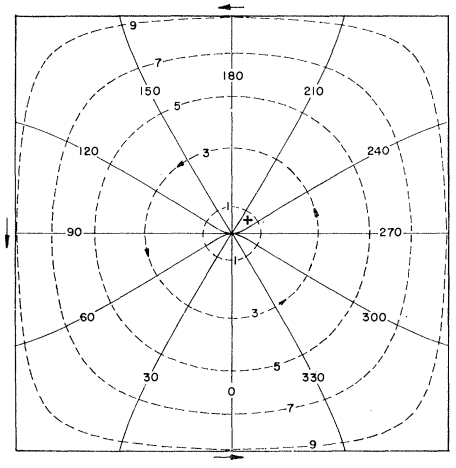

$\tau = 1{\cdot}382,\ k^2 = -1{\cdot}175,\ w = 1,\ \sigma = 0{\cdot}724$

FIGURE 24

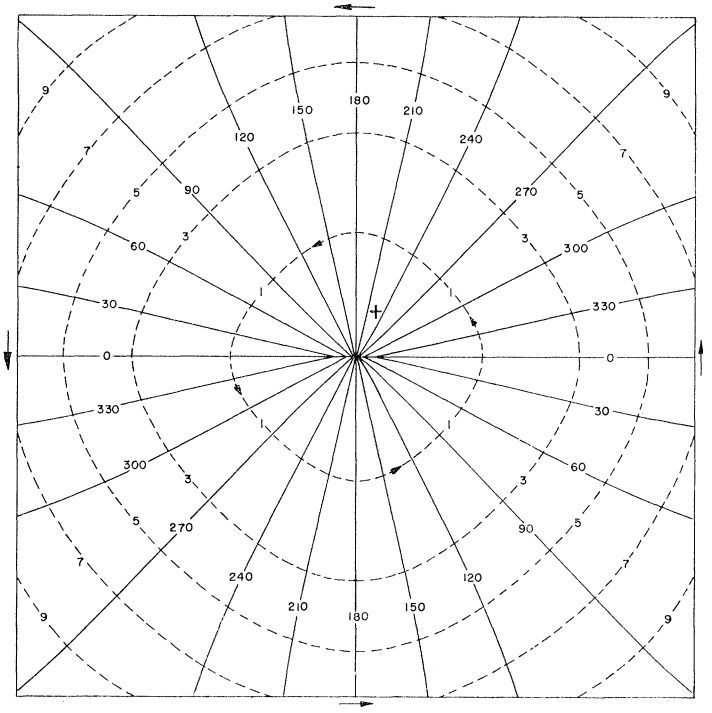

$\tau = 0{\cdot}761,\ k^2 = 1{\cdot}791,\ w = 1,\ \sigma = 1{\cdot}314$

FIGURE 25

FIGURE 24. Free tidal oscillation in a rotating flat square basin. $\tau = 2\omega/\sigma$, $k^2 = (\sigma^2 - 4\omega^2)/gh$. First mode at moderate rotation. Positive wave.

FIGURE 25. Second mode at moderate rotation. Positive wave.

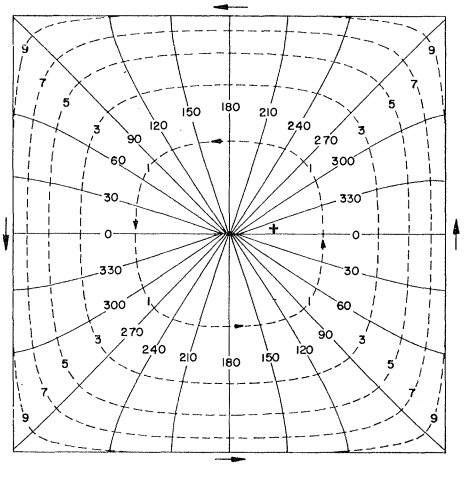

$\tau = 1{\cdot}660,\ k^2 = -6{\cdot}287,\ w = 2,\ \sigma = 1{\cdot}205$

FIGURE 26

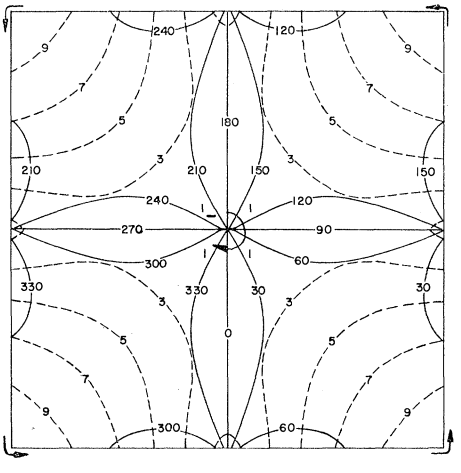

$\tau = 0{\cdot}662,\ k^2 = 3{\cdot}154,\ w = 1,\ \sigma = 1{\cdot}509$

FIGURE 27

FIGURE 26. Second mode at high rotation. Approach to Kelvin regime.

FIGURE 27. Third mode. First appearance near the periphery of four positive amphidromic points in a wave which was negative at lower rotation speeds.

initially with τ, and the other decreasing. The same frequency data are shown in figure 23, where the curves represent the dependence of the characteristic frequency σ on the speed of rotation ω, each expressed in units of ν_1 $(=\frac{1}{2}\pi)$, which is the lowest frequency of tidal oscillation of a square basin in the absence of rotation.

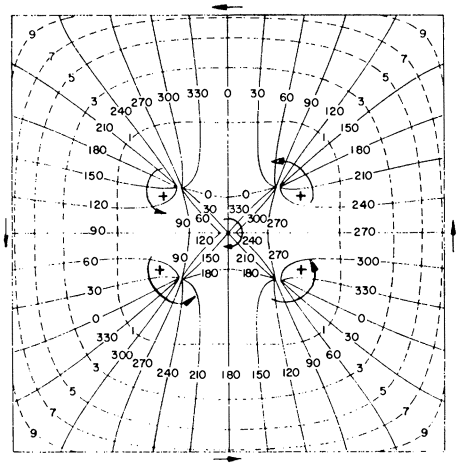

$\tau = 1{\cdot}150,\ k^2 = -2{\cdot}408,\ w = 2, \sigma = 1{\cdot}739$

FIGURE 28

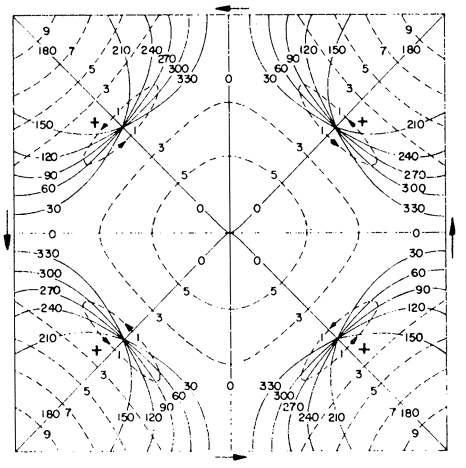

$\tau = 0{\cdot}469,\ k^2 = 8{\cdot}737,\ w = 1,\ \sigma = 2{\cdot}131$

FIGURE 29

FIGURE 28. The mode of figure 27 at higher rotation speeds.

FIGURE 29. The fourth mode at low rotation speeds. Positive wave.

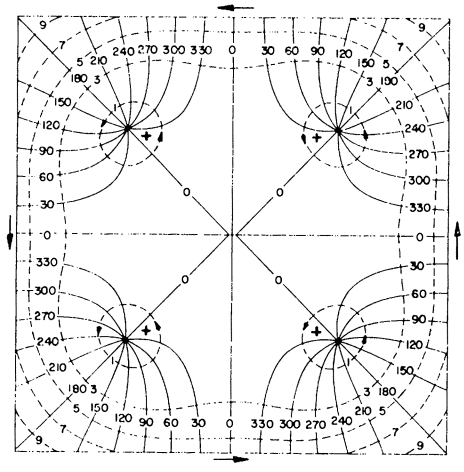

$\tau = 0{\cdot}889,\ k^2 = 2{\cdot}621,\ w = 2,\ \sigma = 2{\cdot}250$

FIGURE 30

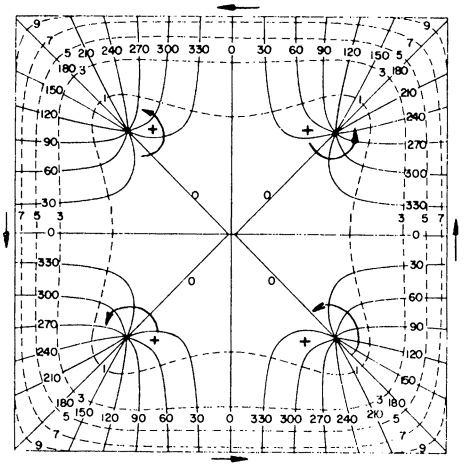

$\tau = 1{\cdot}346,\ k^2 = -9{\cdot}947,\ w = 3,\ \sigma = 2{\cdot}229$

FIGURE 31

FIGURE 30. The fourth mode at moderate rotation. Approach to Kelvin regime. Positive wave.

FIGURE 31. The fourth mode at high rotation. Fully developed Kelvin regime.

The first mode at moderate rotation is shown in figure 24. It consists of a single positive amphidromic system located at the centre. The total change of phase around the periphery of the basin is 2π. Figures 25 and 26 show oscillations in the second mode at moderate and high speeds of rotation respectively. All the above waves are positive. The third mode starts

out with a positive slope at $\tau = 0$, implying a negative wave. As the rotation speed is increased and the curve $k^2(\tau)$ passes the maximum shown in figure 22, four positive amphidromic systems move in from the periphery. This stage is illustrated in figure 27. At higher rotation, shown in figure 28, these positive amphidromic systems move into the interior of the basin, while at the centre the original negative amphidromic point still survives. On the periphery, however, the wave has now turned completely positive. The fourth mode is illustrated in figures 29, 30 and 31. In the last, the Kelvin regime is fully developed, the tidal energy being concentrated mainly near the coast, with little motion in the interior. In figures 25, 28 and 30, the co-tidal lines should pass smoothly through the amphidromic points.

12. Distribution of the tide around a blunt corner

One of the purposes in investigating the tides in basins of the form of circular sectors was to determine the distribution of tides around a corner when the angular opening is greater than π. Such corners were found to retard the convergence in the numerical solution of the tidal equations by the method of finite differences. In the form of the solution we adopted in equation (82), the lowest power of r is r^μ, apart from the constant for $n = 0$. In the neighbourhood of the corner, $r \ll 1$, the solution must satisfy the wave equation

$$(\nabla^2 + k^2)\,\zeta = 0, \tag{88}$$

and the boundary conditions

$$\left(-\frac{1}{r}\frac{\partial}{\partial\theta} - \mathrm{i}\tau\frac{\partial}{\partial r}\right)\zeta = 0, \quad \theta = \pm\frac{\pi}{2\mu}. \tag{89}$$

Taking as a typical solution of (88)

$$\zeta_n = J_\mu(k_n r)\,[\alpha_n \mathrm{e}^{\mathrm{i}\mu\theta} + \beta_n \mathrm{e}^{-\mathrm{i}\mu\theta}], \tag{90}$$

the boundary condition (89) requires that

$$\mu J_\mu(k_n r)\,[\alpha_n \mathrm{e}^{\mathrm{i}\mu\theta} - \beta_n \mathrm{e}^{-\mathrm{i}\mu\theta}] + \tau k_n r \dot{J}_\mu(k_n r)\,[\alpha_n \mathrm{e}^{\mathrm{i}\mu\theta} + \beta_n \mathrm{e}^{-\mathrm{i}\mu\theta}] = 0. \tag{91}$$

On expressing $\dot{J}_\mu(k_n r)$ in terms of Bessel functions of higher order, and retaining the functions of lowest order only, we are led to

$$\zeta_n \simeq J_\mu(k_n r)\,[(\tau-1)\,\mathrm{e}^{\mathrm{i}\mu\theta} + (\tau+1)\,\mathrm{e}^{-\mathrm{i}\mu\theta}]. \tag{92}$$

For the general solution

$$\zeta = \sum_n A_n J_\mu(k_n r)\,[(\tau-1)\,\mathrm{e}^{\mathrm{i}\mu\theta} + (\tau+1)\,\mathrm{e}^{-\mathrm{i}\mu\theta}] \tag{93}$$

we obtain in the vicinity of the origin

$$\zeta \simeq r^\mu[(\tau-1)\,\mathrm{e}^{\mathrm{i}\mu\theta} + (\tau+1)\,\mathrm{e}^{-\mathrm{i}\mu\theta}]\sum_n A_n \frac{k_n^\mu}{2^\mu \mu!}. \tag{94}$$

Equation (94) shows that the singularity near the corner, given by r^μ, is similar to that in potential flow, with the rotation entering only in the expression in brackets, which is regular. Writing (94) in the form

$$\zeta \simeq r^\mu[\tau\cos\mu\theta - \mathrm{i}\sin\mu\theta] \quad (r \ll 1), \tag{95}$$

we should expect to find in (82)

$$-\alpha_1/\beta_1 \simeq \tau. \tag{96}$$

In table 1 we give a comparison of $(-\alpha_1/\beta_1)$ with τ in the solutions obtained for the 270° circular sector ($\mu = \frac{2}{3}$). It is seen that the agreement is good, especially for small values of $|k^2|$.

TABLE 1. VALUES OF $-\alpha_1/\beta_1$, IN THE SOLUTION (82) FOR THE 270° CIRCULAR SECTOR ($\mu = \frac{2}{3}$), COMPARED WITH τ

k^2	τ	$-\alpha_1/\beta_1$
−7·9	1·208	1·35
−7·9	1·333	1·33
−7·9	1·619	1·50
−1·9	1·088	1·087
−1·9	1·171	1·13
−1·9	1·475	1·47
1·1	0·638	0·640
1·1	0·946	0·95
4·1	0·467	0·47
4·1	0·779	0·780
8·1	0·411	0·40
8·1	0·725	0·79
8·1	0·830	0·830
11·2	0·730	0·74
11·2	0·818	0·84
14·5	0·090	0·093
14·5	0·472	0·46

This research was supported by the office of Naval Research under Contract N00014-66-C0080, and by the National Science Foundation under NSF Grant GA-1062.

REFERENCES

Collatz, L. 1965 *The numerical treatment of differential equations*. Chapter 5. New York: Springer-Verlag.

Corkan, R. H. & Doodson, A. T. 1952 *Proc. Roy. Soc.* A **215**, 147.

Davis, P. J. & Rabinowitz, P. 1961 Advances in orthonormalizing computation. *Advances in computers*, vol. 2, pp. 55–133. New York: Academic Press.

Fox, L. (ed.) 1961 *Numerical solution of ordinary and partial differential equations*, p. 301. London: Pergamon Press.

Lamb, H. 1932 *Hydrodynamics*, p. 318. Cambridge University Press.

Poincaré, H. 1910 *Lecons de Mechanique Céleste*, Tome III, p. 299. Paris: Gautier-Villars.

Proudman, J. 1928 *Mon. Not. R. Astr. Soc. Geophys. Suppl.* **2**, 32.

Rao, B. D. 1965 Free gravitational oscillations in rotating rectangular basins. *Tech. Rep.* (NSF-GP-471). *Univ. Chicago, Geophys. Sci.*, no. 18.

Rao, B. D. 1966 *J. Fluid Mech.* **25**, 523.

Taylor, G. I. 1922 *Proc. Lond. Math. Soc.* **20**, 148.

PHILOSOPHICAL TRANSACTIONS OF THE ROYAL SOCIETY A MATHEMATICAL, PHYSICAL & ENGINEERING SCIENCES